

Investigation of electronic and thermal properties of CoCrFe and CoCrFeNi high entropy alloys via extended tight-binding DFT computational method

Fatih Ahmet ÇELİK^{1*}, Sefa KAZANÇ²

¹ Physics Department, Faculty of Arts&Sciences, Bitlis Eren University, Bitlis, Turkey

² Mathematics and Science Education, Faculty of Education, Fırat University, Elazığ, Turkey

*¹facelik@beu.edu.tr, ²skazanc@firat.edu.tr

(Geliş/Received: 18/08/2023;

Kabul/Accepted: 30/11/2023)

Abstract: In this study, CoCrFe and CoCrFeNi transition high entropy alloys (HEAs) are modelled by extended tight-binding density functional theory (DFT) method. Also, the geometric optimizations, band structures, density of states (DOS), thermodynamic properties and phonon dispersion curves of alloys are investigated to give a detailed information. The results show that the covalent d-d bonding between Fe-Cr is occurred because of strong metallic Cr-Fe interactions. The entropy (S) value increases gradually with the addition of Ni element to the CoCrFe alloy. The heat capacity (C_V) increases due to the harmonic effect of the phonons in the range of 0-400 K and then, close to the classic limit at high temperatures with 0.82 J/mol.K and 0.94 J/mol.K for the CoCrFe and the CoCrFeNi. The alloy systems exhibit metallic properties because the DOS of the metals have a nonzero value at the Fermi energy level. Also, the addition of element Ni to the CoCrFe alloy system causes a decrease in phonon frequencies.

Key words: Simulation and modelling, metals and alloys, high entropy alloys, DFT method.

Geniştirilmiş sıkı bağlanma DFT hesaplama yöntemi ile CoCrFe ve CoCrFeNi yüksek entropili alaşımlarının elektronik ve termal özelliklerinin incelenmesi

Öz: Bu çalışmada, CoCrFe ve CoCrFeNi yüksek entropili geçiş alaşımlar (HEA), genişletilmiş sıkı bağlanma yoğunluğu fonksiyonel teorisi (DFT) yöntemi ile modellenmiştir. Ayrıca, modellenen alaşımların geometrik optimizasyonları, bant yapıları, durum yoğunlukları (DOS), termodinamik özellikleri ve fonon dağılım eğrileri incelenmiştir. Sonuçlar Fe-Cr arasındaki kovalent d-d bağının, güçlü metalik Cr-Fe etkileşimleri nedeniyle oluştuğunu göstermektedir. CoCrFe alaşımına Ni elementinin eklenmesiyle entropi değeri kademeli olarak artmakla beraber ve 0-400 K aralığında fononların harmonik etkisine bağlı olarak ısı kapasitesi artmakta ve daha sonra CoCrFe için 0,82 J/mol.K ve 0,94 J/mol.K ile yüksek sıcaklıklarda klasik sınıra yaklaşmaktadır. CoCrFeNi. Alaşım sistemleri metalik özellikler sergiler çünkü metallerin DOS'ları Fermi enerji seviyesinde sıfırdan farklı bir değere sahiptir. Ayrıca CoCrFe alaşım sistemine Ni elementinin eklenmesi fonon frekanslarında azalmaya neden olmaktadır.

Anahtar kelimeler: Simülasyon ve modelleme, metaller ve alaşımlar, yüksek entropili alaşımlar, DFT yöntemi.

1. Introduction

In recent years, high entropy alloys (HEAs) have attracted extensive attentions of researchers because of their remarkable physical characteristics. Especially, HEAs including equiatomic multicomponent enables to develop in material design and engineering technologies [1-6]. Because HEAs with adding more different elements have important mechanical properties such as strength, ductility, corrosion resistance [1-10]. In this context, CoCrFeNi, CoCrFeMnNi, CoFeNi, CoCrNi HEAs have been investigated to understand the mechanical and structural properties of HEAs via experimental analysis [11-15]. Among them, Li et al. [10] introduced the non-equiatomic CoCrFeMnNi HEAs which exhibited excellent strength and ductility. Ji et al. [16] studied the CoCrCuFeNi for understanding the wear resistance properties. Zhang et al. investigated the deformation behaviors of a dual-phase FeCoCrNiMn alloy with transformation-induced plasticity effect [15]. The microstructures and mechanical properties of CoCrFeMnNi HEAs with addition of nitrogen alloying during different heat treatments were systematically studied by Xiong et al [7].

These experimental studies reveal that the addition of Fe and Ni elements to CoCr/CuMn can affect phase formations behavior, electronic properties, and mechanical characteristics of these alloys [1-5]. Although experimental studies are available on HEAs, there have been still needed powerful computational approaches to overcome difficulties arising from experimental studies. Hence, many researchers recently have studied on HEAs to reveal the mechanical properties and microstructure of HEAs by using computational methods. Sharma et al.

* Corresponding author: facelik@beu.edu.tr. ORCID Number of authors: ¹ 0000-0001-7860-5550, ² 0000-0002-8896-8571

explored the structural phase transformations in AlxCrCoFeNi using classical molecular dynamics (MD) with classical Lennard-Jones pair-potentials [17]. Similarly, Liu reported a MD study which performed to mechanical characteristics and homogeneous plastic inception of CoCrCuFeNi HEAs under uniaxial tension [18]. Besides classical MD studies, density functional theory (DFT) methods are used in model calculations to evaluate physical properties of HEAs [19]. Biermair et al. demonstrated the applicability of a DFT for prediction of the lattice constant and thermodynamic property changes of a paramagnetic HEAs [20]. Moreover, some thermo-physical properties of NiFeCrCo were investigated via first-principles tool by Niu et al [21].

As it appears from quantum mechanical calculations, Cr/Fe interactions are a notable factor for realizing the electronic band structure because of the covalent d-d bonding between Cr and Fe d states [19]. For this purpose, density functional theory (DFT) methods provide an accurate description the different properties of the material's [22-27]. Among these, GFN1-xTB supplies higher accuracy for all combination of periodic table [28]. But there is still a lack of geometric optimization, band structures, phonon spectrum properties and density of states (DOS) by using extended tight-binding DFT with SCC contributions of CoCrFe and CoCrFeNi HEAs alloys. In the current work, we reported a computational exploration of CoCrFe and CoCrFeNi HEAs by using extended tight-binding DFT method. We have calculated the band structures, DOS, phonon spectrum and some thermodynamic parameters of alloys.

2. Material and Method

A new extended tight-binding method (GFN1-xTB) provides to enough accuracy for geometry optimizations. The total energy expression comprises electronic (*el*), atom pairwise repulsion (*rep*), dispersion (*disp*), and halogen-bonding (XB) terms [28]:

$$E = E_{el} + E_{rep} + E_{disp} + E_{XB} \quad (1)$$

The electronic energy E_{el} is given by

$$E_{el} = \sum_i^{occ} n_i \langle \varphi_i | H_0 | \varphi_i \rangle + \frac{1}{2} \sum_{A,B} \sum_{l(A)} \sum_{l'(B)} p_l^A p_{l'}^B \gamma_{AB,ll'} + \frac{1}{3} \sum_A \tau_A q_A^3 - T_{el} S_{el} \quad (2)$$

where φ_i are the valence molecular orbitals with occupation numbers n_i and H_0 is the zero-order Hamiltonian. $T_{el} S_{el}$ is the electronic free energy term [28]. GFN1-xTB, based on developed extended tight-binding method, aims to reduce set of physically interpretative parameters to solve the distinct deficiencies of other DFT calculations by making a parameterization in a wide range of elements up to $Z=86$. Hence, this method has been recently used for understanding the optimization process of various materials at nano-scale [28]. Using the symmetry properties, firstly, the CoCr crystal structure was built according to $Pm\bar{3}m$ space group with the following unit cell lattice parameters: $a = b = c = 2.821 \text{ \AA}$. Fig. 1 shows the atomic distribution on the lattice points of Cu-%50Cr alloy system containing 128 atoms. Fe and Ni atoms were doped on the crystal lattice by creating a random mixture of elements, respectively. The CoCrFe and CoCrFeNi model systems were created to form crystal phase. The geometric optimizations are performed using the Amsterdam Modeling Suite (AMS) software (version 2020.104) [29-31] with DFTB module based on GFN1-xTB calculations. The maximum force and energy convergence are executed as 0.001 Ha/\AA and $1 \times 10^{-5} \text{ Ha}$ on each atom with 0.001 \AA step convergence until the lattice constants and the atomic positions are relaxed during the geometric optimization process. The stress energy per atom during the optimized lattice is set up $5 \times 10^{-5} \text{ Ha}$.

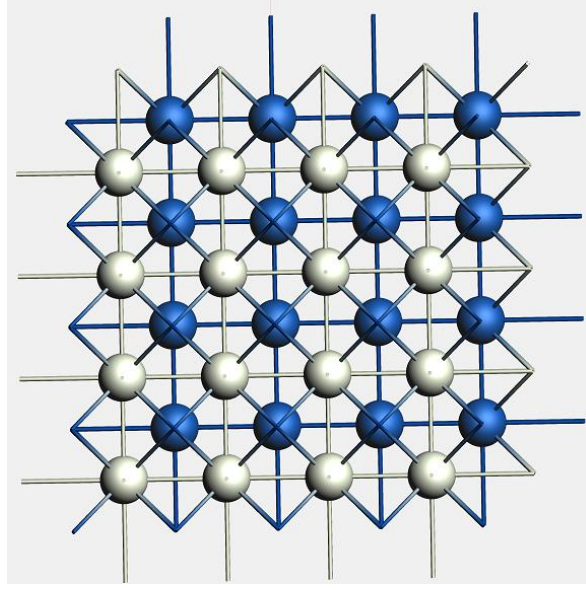


Figure 1. Crystal structure of CoCr.

3. Results and Discussion

Fig. 2 (a) and Fig. 3 (a) show the evolution of the total energy with respect to the frame number or optimization iteration step for CuCrFe and CuCrFeNi systems, respectively. The total energy for the systems has the maximum value at the beginning of optimization. The energy reaches its minimum with progressing of optimization process. The systems have high stability at final of optimization compared with the beginning structure and also, the energy of CoCrFe is lower than CoCrFeNi during the optimization process. The volumes of systems during the optimization process are shown in Fig. 2 (b) and Fig. 3 (b). The figures show that the volumes of systems linearly increase at the beginning of optimization and then dramatically decrease at certain optimization step. Then, the system volumes reach a stable value after iteration 60. Fig. 2 (c, d) and Fig. 3 (c, d) show the atomic configurations of CuCrFe and CuCrFeNi structures at the beginning and final of optimization. From the figures, we can see that Fe and Cr atoms tend to bond during the optimization. This result can be explicated that covalent d–d bonding between Fe–Cr is evidenced because of strong metallic Cr–Fe interactions. This strong bonding interaction between Cr–Fe for electron exchange and correlation early investigated by Johnson et. al by using DFT [19].

Investigation of electronic and thermal properties of CoCrFe and CoCrFeNi high entropy alloys via extended tight-binding DFT computational method

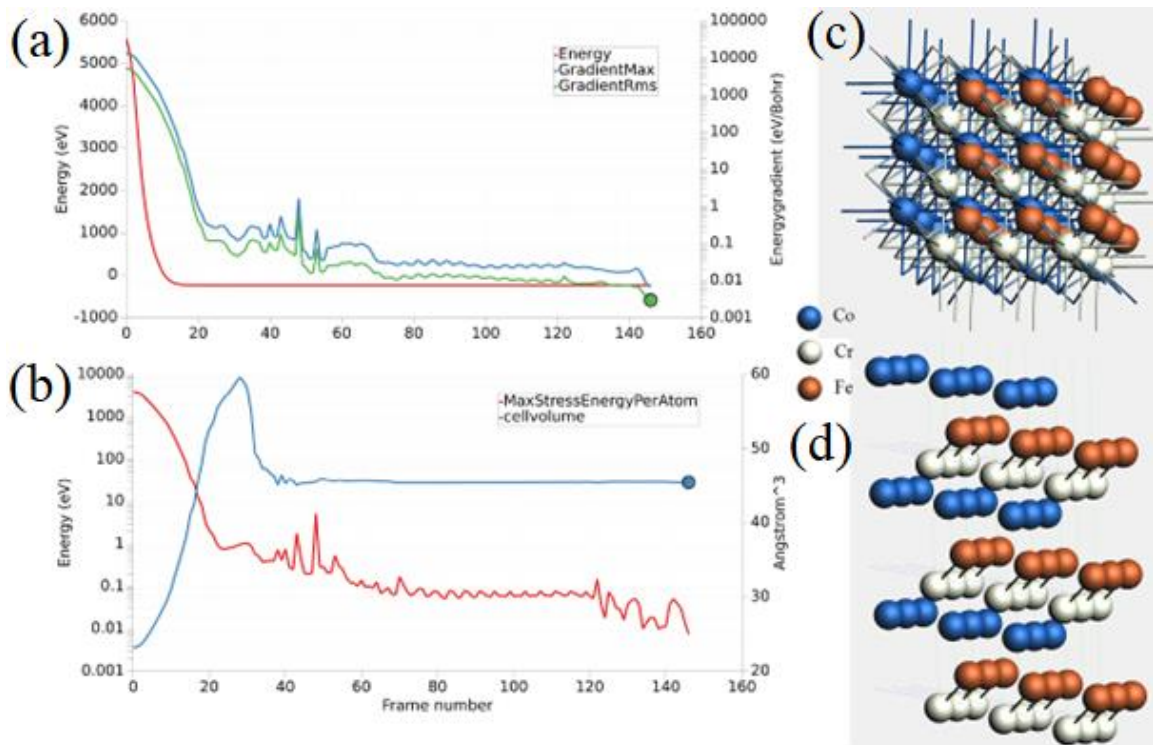


Figure 2. Geometric optimization process of CoCrFe.

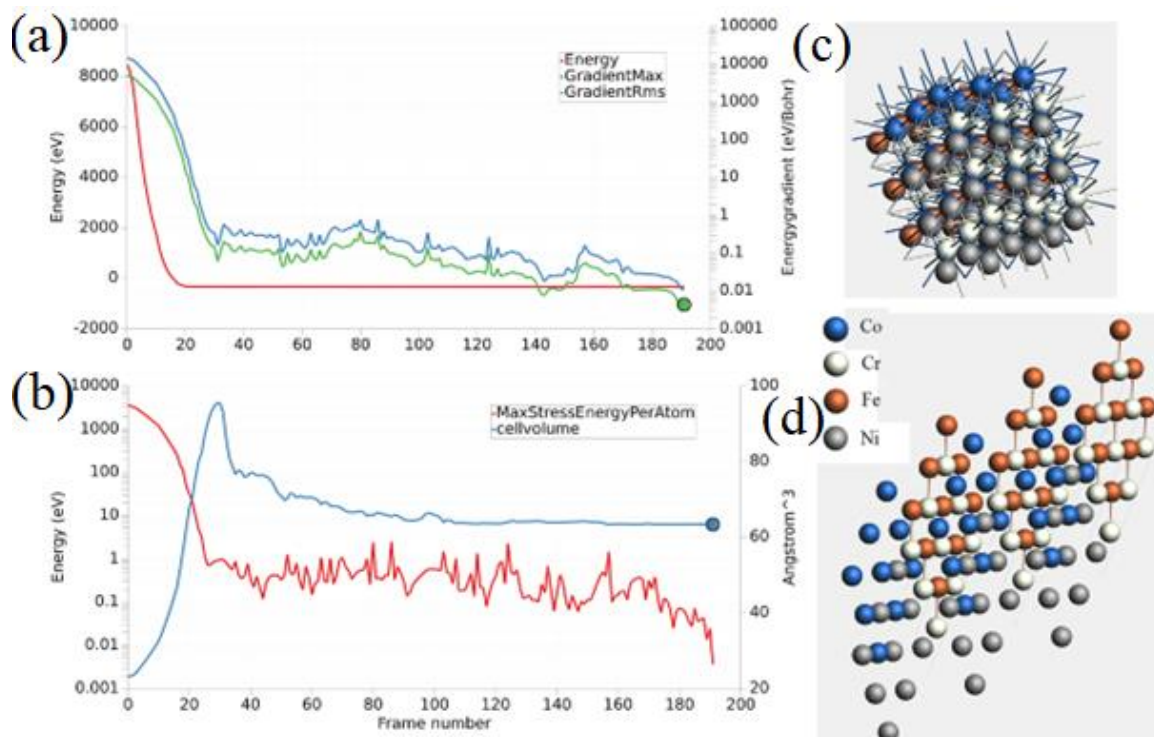


Figure 3. Geometric optimization process of CoCrFeNi.

The variation of thermodynamic parameters obtained from phonon as shown in Fig. 4 (a-d). The internal energies of both alloys increase linearly in the temperature range of 50-1000 K. It is noted that the internal energy of CoCrFe at 0 K is lower than the internal energy of CoCrFeNi. When the variation graph of free energy according to temperature is examined in Fig. 4 (b), it is seen that the free energy is at an almost constant value in both alloy systems up to 50 K, however, it exhibits a linear decrease with the increase in temperature. The entropy values calculated in the low temperature region increase rapidly with the increase in temperature as seen Fig. 4 (c). This increment continues exponentially as the contribution of vibration to entropy (S) increases as the temperature rises [32, 33]. The increase continues exponentially as the contribution of vibration to entropy increases as the temperature continues to rise. It is observed that the entropy value increases gradually with the addition of Ni element to the CoCrFe alloy. From figure, the C_V increases due to the harmonic effect of the phonons in the range of 0-400 K. The T^3 dependence at low temperatures is detailed in Figure 4 (d). This increase is strongly dependent on temperature. But, when the temperature is higher than 400 K, the C_V is close to the classic limit in good agreement with Dulong-Petit's law [34] at about 0.82 J/mol.K and 0.94 J/mol.K for the CoCrFe and the CoCrFeNi, respectively.

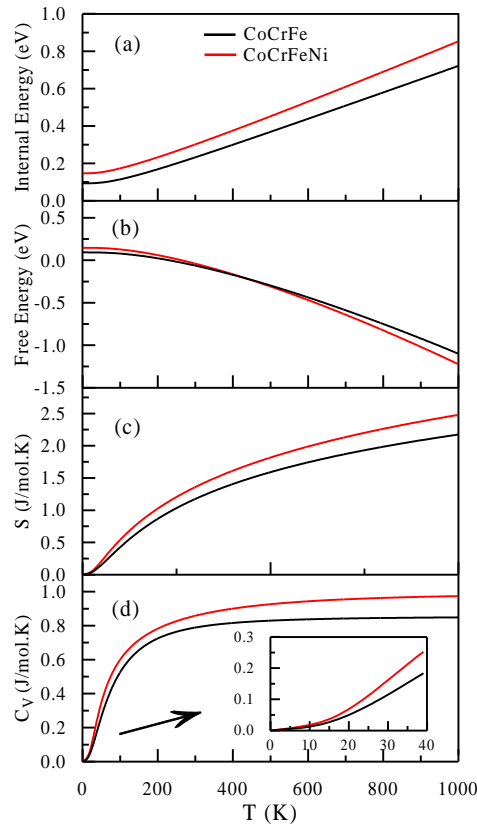


Figure 4. Thermodynamic parameters of model systems (a) internal energy (b) free energy (c) entropy (d) heat capacity.

Fig. 5 and Fig.6 show the band structure of systems. It is clearly observed that there is no band gap formation along the high symmetry lines at the Fermi energy level for both alloys. In other words, the top of the valence band and the bottom of the conduction band overlap. This causes the curve to have a value above zero at the Fermi energy level in the DOS. It could be argued that because the DOS of the metals have a nonzero value at the Fermi energy level, both alloy systems exhibit metallic properties. Since most of the occupied states come from the d states of Co, Cr, Fe and Ni atoms, it could be argued that the d orbitals make the major contribution to DOS in the energy band structure [35]. The $4s^2 3d^7$, $4s^1 3d^5$, $4s^2 3d^6$ and $4s^2 3d^8$ orbitals of Co, Cr, Fe and Ni elements are considered as valence states, respectively. These elements tend to form covalent bonds with each other because of their 3d electrons. In Figure 6, a small band gap formation is observed in the energy band structure in the $A5-\Gamma$ -

A6 high symmetry directions of the CoCrFeNi alloy system. This band gap causes a decrease in DOS. Although band gap is formed in some aspects of the Brillouin zone, there are sufficiently high DOS at the Fermi level to make the CoCrFeNi alloy system metallic [36]. It is clearly observed from the band structure in figure that the p states are filled well above the conduction band because of the addition of Ni element to the CoCrFe alloy system. In addition, it is determined that the s and p states also contribute to the DOS in the valence band and conduction band.

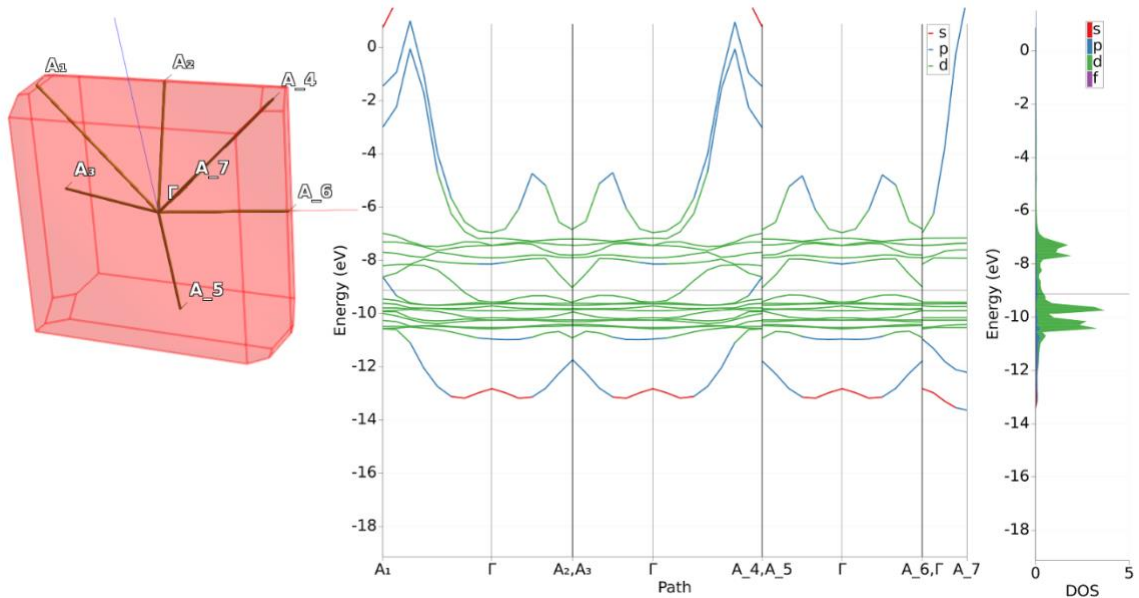


Figure 5. Band structure of CoCrFe.

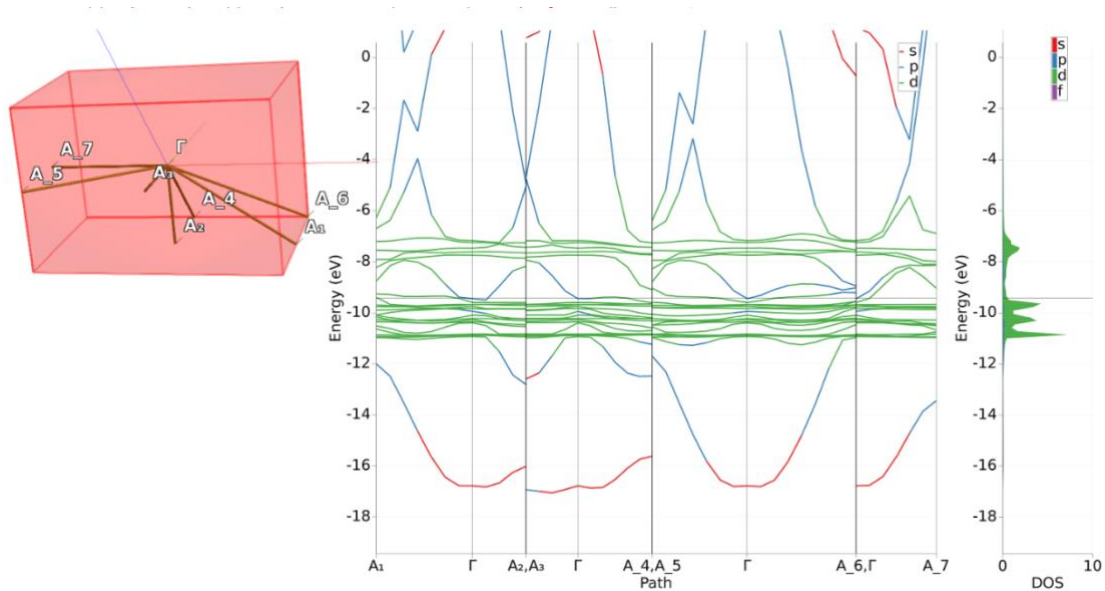


Figure 6. Band structure of CoCrFeNi.

In order to understand the lattice dynamics microscopically, it is required to know the phonon distribution. Phonon properties of solids are very important because they are closely related to various fundamental properties such as thermal expansion, specific heat, electron-phonon interaction, and thermal conduction by lattice [37]. According to the lattice vibration theory, there are $3n$ number of phonon arms in a crystal with n number of atoms per unit cell. These phonon arms consist of 3 acoustic arms and $3n-3$ optical arms [38]. In order to verify the dynamic stability of CoCrFe and CoCrFeNi high entropy alloy systems, phonon dispersion curves were calculated along the path containing the high symmetry points of the Brillouin region, as seen in Fig. 7 and Fig. 8. There are 3 atoms in the primitive unit cell of the $Pm\bar{3}m$ alloy model with space group symmetry. Thus, it is observed that the phonon spectrum has a total of 9 branches, 3 being acoustic modes and 6 being optical modes. In a stable crystal structure, all phonon frequencies must be positive [39]. It was determined that the phonon frequencies obtained for both alloy systems were positive along the high symmetry directions of the Brillouin region, in other words, no imaginary phonon frequencies were observed. This clearly indicates that both alloy systems are dynamically stable [37, 38, 40].

It is clearly observed in figures that the addition of element Ni to the CoCrFe alloy system causes a decrease in phonon frequencies. It is known that high-frequency phonon modes originate mainly from light atoms, while low-frequency phonon modes originate from heavier atoms [39]. Therefore, it can be argued that the addition of Ni element to the CoCrFe alloy system causes a decrease in phonon frequencies. It is observed that the gaps between the optical and acoustic phonon modes in the phonon distribution curves of both alloy systems are very small or does not exist in some high symmetry directions, and they intersect with each other at more than one Brillouin zone point. It can be argued that this is an indication of the high entropy alloy systems used in the study exhibiting a ductile structure [41]. There are many studies in the literature in which ductility is analyzed by associating it with phonon dispersion [42-46]. However, in Figure 8, the formation of a frequency gap between the optical and acoustic arms in the phonon distribution curve in the $A5-\Gamma-A6$ high symmetry directions of the CoCrFeNi alloy system is clearly observed. When the energy band structure of the same alloy system is examined in Figure 2, it can be determined that a small band gap is formed in the same high symmetry directions. Although there is a frequency gap in these directions of the Brillouin zone, this does not affect the dynamic stability of the system. In addition, the frequency gap can be directly related to the mass ratio of atoms in the model system. A higher mass ratio indicates a larger frequency interval [37].

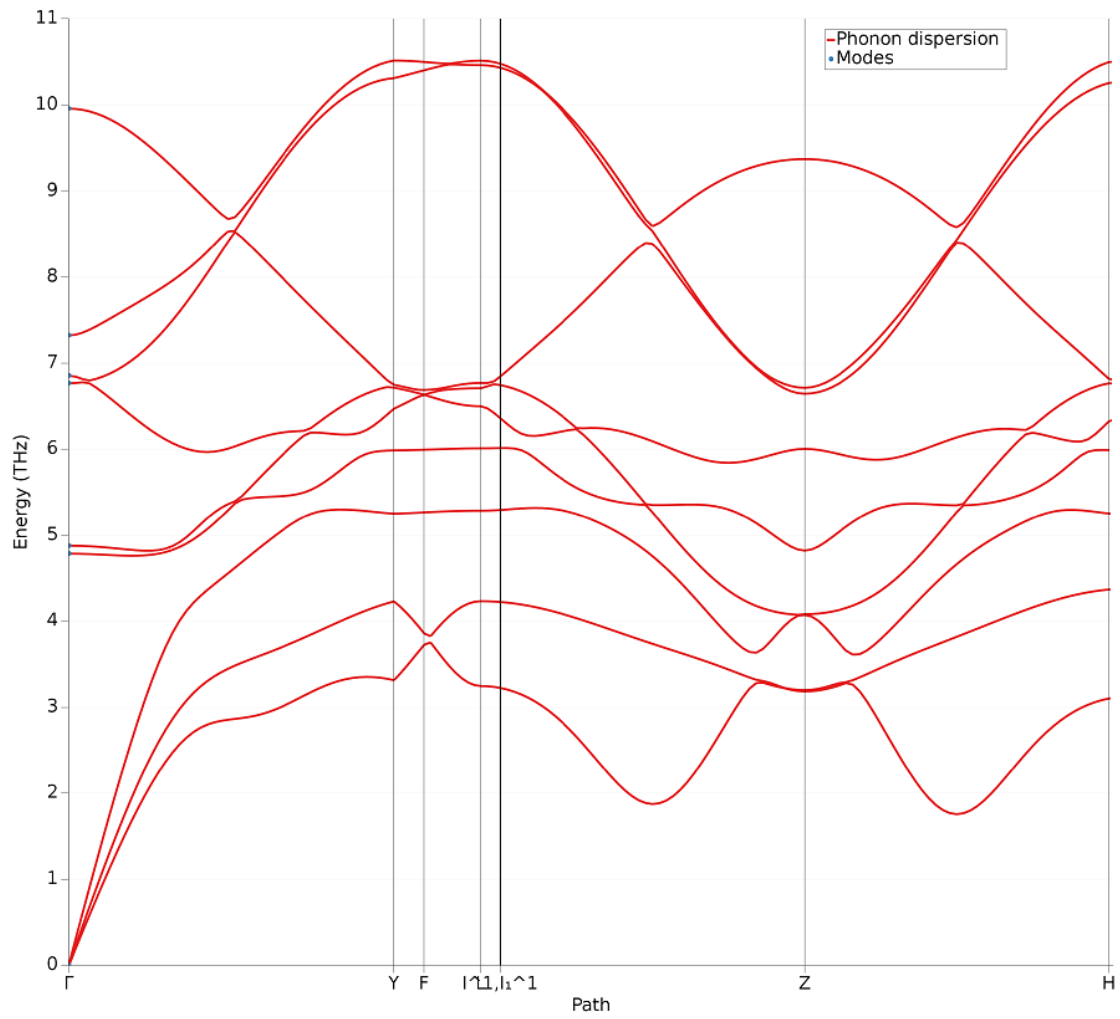


Figure 7. Phonon curves of CoCrFe.

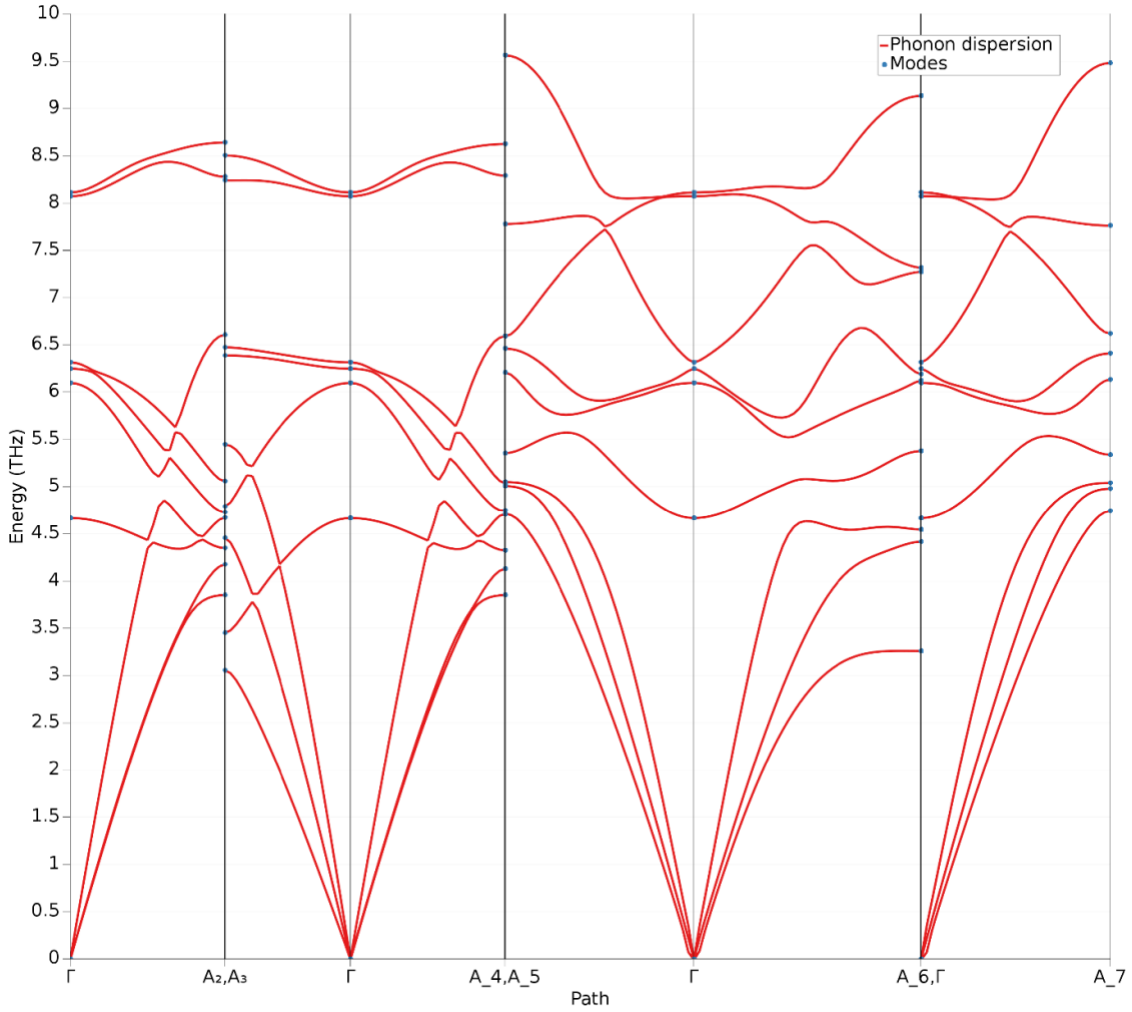


Figure 8. Phonon curves of CoCrFeNi.

4. Conclusion

In summary, we have performed tight-binding DFT calculations of CoCrFe and CoCrFeNi HEAs. The geometric optimization, electronic and thermodynamic properties have also been investigated. Fe and Cr atoms tend to bond during the optimization because of strong metallic Cr–Fe interactions. Cv values are obtained as 0.82 J/mol.K and 0.94 J/mol.K for the CoCrFe and the CoCrFeNi. Moreover, there is no band gap formation along the high symmetry lines at the Fermi energy level for both alloys due to exhibit metallic properties of systems. the gaps between the optical and acoustic phonon modes in the phonon distribution curves of both alloy systems are very small and does not exist in some high symmetry directions.

References

- [1] Zhao S, Li Z, Zhu C, Yang W, Zhang Z, Armstrong DE., Meyers MA. Amorphization in extreme deformation of the CrMnFeCoNi high-entropy alloy. *Sci Adv* 2021; 7(5): eabb3108.
- [2] Yang YC, Liu C, Lin CY, Xia Z. Core effect of local atomic configuration and design principles in AlxCoCrFeNi high-entropy alloys. *Scr Mater* 2020; 178: 181-186.
- [3] Fan AC, Li JH, Tsai MH. On the phase constituents of three CoCrFeNiX (X= Cr, Mo, W) high-entropy alloys after prolonged annealing. *Mater Chem Phys* 2022; 276: 125431.
- [4] Lin Y, Yang T, Lang L, Shan C, Deng H, Hu W, Gao, F. Enhanced radiation tolerance of the Ni-Co-Cr-Fe high-entropy alloy as revealed from primary damage. *Acta Mater* 2020; 196: 133-143.
- [5] Daryoush S, Mirzadeh H, Ataie A. Amorphization, mechano-crystallization, and crystallization kinetics of mechanically alloyed AlFeCuZnTi high-entropy alloys. *Mater Lett* 2022; 307: 131098.
- [6] Fang W, Chang R, Ji P, Zhang X, Liu B, Qu X, Yin F. Transformation induced plasticity effects of a non-equal molar Co-Cr-Fe-Ni high entropy alloy system. *Metals* 2018; 8(5): 369-379
- [7] Xiong F, Fu R, Li Y, Xu B, Qi X. Influences of nitrogen alloying on microstructural evolution and tensile properties of CoCrFeMnNi high-entropy alloy treated by cold-rolling and subsequent annealing. *Mater Sci Eng A* 2020; 787: 139472.
- [8] He F, Wang Z, Wu Q, Niu S, Li J, Wang J, Liu CT. Solid solution island of the Co-Cr-Fe-Ni high entropy alloy system. *Scr Mater* 2017; 131: 42-46.
- [9] Feng R, Zhang C, Gao MC, Pei Z, Zhang F, Chen Y, Liaw PK. High-throughput design of high-performance lightweight high-entropy alloys. *Nat Commun* 2021; 12(1): 1-10.
- [10] Li Z. Interstitial equiatomic CoCrFeMnNi high-entropy alloys: carbon content, microstructure, and compositional homogeneity effects on deformation behavior. *Acta Mater* 2019; 164: 400-412.
- [11] Zhang Z, Jiang Z, Xie Y, Chan SLI, Liang J, Wang J. Multiple deformation mechanisms induced by pre-twinning in CoCrFeNi high entropy alloy. *Scr Mater* 2022; 207: 114266.
- [12] Zaddach AJ, Niu C, Koch CC, Irving DL. Mechanical properties and stacking fault energies of NiFeCrCoMn high-entropy alloy. *Jom* 2013; 65(12): 1780-1789.
- [13] Vaidya M, Karati A, Marshal A, Pradeep KG, Murty BS. Phase evolution and stability of nanocrystalline CoCrFeNi and CoCrFeMnNi high entropy alloys. *J Alloys Compd* 2019; 770: 1004-1015.
- [14] Fang W, Yu H, Chang R, Zhang X, Ji P, Liu B, Yin F. Microstructure and mechanical properties of Cr-rich Co-Cr-Fe-Ni high entropy alloys designed by valence electron concentration. *Mater Chem Phys* 2019; 238: 121897.
- [15] Zhang T, Zhao RD, Wu FF, Lin SB, Jiang SS, Huang YJ, Eckert J. Transformation-enhanced strength and ductility in a FeCoCrNiMn dual phase high-entropy alloy. *Mater Sci Eng A* 2020; 780: 139182.
- [16] Ji, X, Ji C, Cheng J, Shan Y, Tian S. Erosive wear resistance evaluation with the hardness after strain-hardening and its application for a high-entropy alloy. *Wear* 2018; 398: 178-182.
- [17] Sharma A, Deshmukh SA, Liaw PK, Balasubramanian G. Crystallization kinetics in AlxCrCoFeNi (0 ≤ x ≤ 40) high-entropy alloys. *Scr Mater* 2017; 141: 54-57.
- [18] Liu J. Molecular dynamic study of temperature dependence of mechanical properties and plastic inception of CoCrCuFeNi high-entropy alloy. *Phys Lett A* 2020; 384: 126516.
- [19] Johnson DF, Jiang DE, Carter EA. Structure, magnetism, and adhesion at Cr/Fe interfaces from density functional theory. *Surf Sci* 2007; 601(3): 699-705.
- [20] Biermair F, Razumovskiy VI, Ressel G. Influence of alloying on thermodynamic properties of AlCoCrFeNiTi high entropy alloys from DFT calculations. *Comput Mater Sci* 2022; 202: 110952
- [21] Niu C, Zaddach AJ, Koch CC, Irving DL. First principles exploration of near-equiatomic NiFeCrCo high entropy alloys. *J Alloys Compd* 2016; 672: 510-520.
- [22] Kohn W, Sham LJ. Self-Consistent Equations Including Exchange and Correlation Effects. *Phys Rev* 1965; 140: A1133-A1138.
- [23] Galvão BR, Viegas LP, Salahub DR, Lourenço MP. Reliability of semiempirical and DFTB methods for the global optimization of the structures of nanoclusters. *J Mol Model* 2020; 26(11): 1-8.
- [24] Wahiduzzaman M, Oliveira AF, Philipsen P, Zhechkov L, Van Lenthe E, Wittek HA, Heine T. DFTB parameters for the periodic table: Part I, electronic structure. *J Chem Theory Comput* 2013; 9(9): 4006-4017.
- [25] Chopra S. Performance study of the electronic and optical parameters of thermally activated delayed fluorescence nanosized emitters (CCX-I and CCX-II) via DFT, SCC-DFTB and B97-3c approaches. *J Nanostruct Chem* 2020; 10: 115-124.
- [26] Slater JC, Koster GF. Simplified LCAO method for the periodic potential problem. *Phys Rev* 1954; 94(6): 1498.
- [27] Yildiz AK, Celik FA. Atomic concentration effect on thermal properties during solidification of Pt-Rh alloy: A molecular dynamics simulation. *J Cryst Growth* 2017; 463: 194-200.
- [28] Grimme S, Bannwarth C, Shushkov P. A robust and accurate tight-binding quantum chemical method for structures, vibrational frequencies, and noncovalent interactions of large molecular systems parametrized for all spd-block elements (Z= 1-86). *J. Chem Theory Comput* 2017; 13(5): 1989-2009.

- [29] Te Velde GT, Bickelhaupt FM, Baerends EJ, Fonseca Guerra C, van Gisbergen SJ, Snijders JG, Ziegler T. Chemistry with ADF. *J Comput Chem* 2001; 22(9): 931-967.
- [30] Fonseca Guerra C, Snijders JG, Te Velde GT, Baerends EJ. Towards an order-N DFT method. *Theor Chem Acc* 1998; 99(6): 391-403.
- [31] AMS DFTB 2021.1, SCM, Theoretical Chemistry, Vrije Universiteit Amsterdam, The Netherlands, 2013 <http://www.scm.com>.
- [32] Jain E, Pagare G, Dubey S, Sharma R, Sharma Y. High pressure phonon and thermodynamic properties of Ru based intermetallics: A DFT investigation. *J Phys Chem Solids* 2018; 122: 246-254.
- [33] Asadi Y, Nourbakhsh Z. First principle characterization of structural, electronic, mechanical, thermodynamic, linear and nonlinear optical properties of zinc blende InAs, InSb and their InAs_xSb_{1-x} ternary alloys. *J Phys Chem Solids* 2019; 132: 213-221.
- [34] Arıkan N, İyigör A, Candan A, Uğur Ş, Charifi Z, Baaziz H, Uğur G. Structural, elastic, electronic and phonon properties of scandium-based compounds ScX₃ (X= Ir, Pd, Pt and Rh): An ab initio study. *Comput Mater Sci* 2013; 79: 703-709.
- [35] Rameshkumar S, Jaiganesh G, Jayalakshmi V. Structural, phonon, elastic, thermodynamic and electronic properties of Mg–X (X= La, Nd, Sm) intermetallics: The first principles study. *J Magnes Alloy* 2019; 7(1): 166-185.
- [36] Mukherjee D, Sahoo BD, Joshi KD, Gupta SC. High pressure phase transition in Zr–Ni binary system: A first principle study. *J Alloys Compd* 2015; 648: 951-957.
- [37] Jain E, Pagare G, Dubey S, Sharma R, Sharma, Y. High pressure phonon and thermodynamic properties of Ru based intermetallics: A DFT investigation. *J Phys Chem Solids* 2018; 122: 246-254.
- [38] Yang JW, An L, Zheng JJ. Structure, mechanical and phonon stability of the Th–Sn system from ab initio. *J Nucl Mater* 2021; 556: 153187.
- [39] Zhao Y, Li H, Huang Y. The structure, mechanical, electronic and thermodynamic properties of bcc Zr–Nb alloy: A first principles study. *J Alloys Compd* 2021; 862: 158029.
- [40] Guechi A, Chegaar M, Bouhemadou A, Arab F. Structural, mechanical and phonons properties of binary intermetallic compound BaSn₃ under pressure. *Solid State Commun* 2021; 323: 114110.
- [41] Liu J, Guo X, Lin Q, He Z, An X, Li L, Zhang Y. Excellent ductility and serration feature of metastable CoCrFeNi high-entropy alloy at extremely low temperatures. *Sci China Mater* 2019; 62(6): 853-863.
- [42] Arıkan N, Charifi Z, Baaziz H, Uğur Ş, Ünver H, Uğur G. Electronic structure, phase stability, and vibrational properties of Ir-based intermetallic compound IrX (X= Al, Sc, and Ga). *J Phys Chem Solids* 2015; 77: 126-132.
- [43] Parlinski K, Li ZQ, Kawazoe Y. First-principles determination of the soft mode in cubic ZrO₂. *Phys Rev Lett* 1997; 78(21): 4063.
- [44] Wang R, Wang S, Wu X, Liu A. First-principles phonon calculations of thermodynamic properties for ductile rare-earth intermetallic compounds. *Intermetallics* 2011; 19(10): 1599-1604.
- [45] Perdew JP, Burke K, Ernzerhof M. Generalized gradient approximation made simple. *Phys. Rev. Lett* 1996; 77(18): 3865.
- [46] Blanco MA, Francisco E, Luana V. GIBBS: isothermal-isobaric thermodynamics of solids from energy curves using a quasi-harmonic Debye model. *Comput Phys Commun* 2004; 158(1): 57-72.